Ecological Indicators 166 (2024) 112266

Contents lists available at ScienceDirect

Ecological Indicators

journal homepage: www.elsevier.com/locate/ecolind

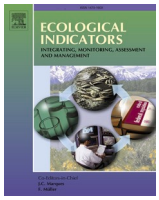

Original Articles

Fractional Richness: An index for camera trap networks

Laura Marie Berman [a,b,1,*], Fabian D Schneider [b,2], Ryan P. Pavlick [b,3], Jennifer Stenglein [c,4], Ryan Bemowski [c,5], Morgan Dean [b,d,6], Philip A Townsend [a,7]

[a] University of Wisconsin–Madison, Madison, WI, USA
[b] Jet Propulsion Laboratory, California Institute of Technology, CA, USA
[c] Wisconsin Department of Natural Resources, WI, USA
[d] University of California, Los Angeles, Los Angeles, CA, USA

ARTICLE INFO

Keywords:
Fractional Richness
Detectability
Camera trapping

ABSTRACT

Camera trapping networks have the potential to monitor wildlife diversity at large scales. However, their efficacy in detecting different species varies, leading to considerable disparities in population density estimates. Furthermore, species of different trophic levels and body sizes naturally occur at different densities, challenging the evenness assumptions inherent in conventional diversity indices. Here we present a novel index: Fractional Richness, which is specifically designed for application in extensive camera trap networks. The index addresses situations where evenness is uninformative, for example in communities characterized by multiple trophic levels, diverse body sizes, variable population densities, or other complications. To determine the effectiveness of our Fractional Richness index, we modeled spatial patterns of Shannon diversity, species richness, and Fractional Richness for two wildlife communities in Wisconsin USA to quantitatively measure which index best reflected ecologically relevant landscape patterns. One community was much more uneven than the other, with detection rates ranging across three orders of magnitude. The more even community could be modeled accurately with both Shannon diversity and Fractional Richness, but the highly uneven community could only be modeled accurately with Fractional Richness. Maximum population density varies by species, and most wildlife survey methods are not equally capable of detecting all species. In communities with both high and low-density species, or when detectability varies, evenness may not be the most informative measure. In these situations, Fractional Richness may be a more suitable index.

1. Introduction

Understanding where species diversity is highest, and what factors facilitate high diversity in an ecosystem, is a high priority question in the field of conservation ecology. Measuring global declines in species diversity, shifts in community abundances, and successfully assessing progress towards conservation and restoration goals all depend on reliable and intuitive indexes of diversity. However, typical indexes neglect a key aspect of ecosystem health: population density and decline. Species across plant and animal taxa are suffering from population declines on a global scale, and the field of ecology would benefit from an index which measures the robustness of populations in a community, in addition to traditional measures like Shannon diversity and species richness. Typical diversity indexes which incorporate measures of evenness also struggle to intuitively predict wildlife diversity when not all species are equally easily detected, or when maximum population density varies between species. Using megafauna in the state of Wisconsin, USA, as a case study, we present a novel index which is sensitive

* Corresponding author at: University of Wisconsin–Madison, Madison, Wisconsin, USA.
E-mail address: lberman6@wisc.edu (L.M. Berman).
[1] orcid.org/0000-0002-4080-2361.
[2] orcid.org/0000-0003-1791-2041.
[3] orcid.org/0000-0001-8772-3508.
[4] orcid.org/0000-0003-4578-5908.
[5] orcid.org/0009-0001-3259-7513.
[6] orcid.org/0009-0002-3020-0508.
[7] orcid.org/0000-0001-7003-8774.

https://doi.org/10.1016/j.ecolind.2024.112266
Received 22 March 2024; Received in revised form 14 June 2024; Accepted 17 June 2024
Available online 27 June 2024

to population declines and can be used effectively when evenness proves uninformative.

1.1. Modeling diversity in large camera trap networks

The use of camera traps has increased exponentially in recent decades (Burton et al., 2015) with camera trapping networks established across the globe (e.g. Ahumada et al., 2011, McShea et al., 2016) and ongoing efforts to coordinate existing camera trapping efforts into still larger networks (Steenweg et al., 2017, Cove et al., 2021). This study uses data from Snapshot Wisconsin, a network of camera traps deployed throughout WI, USA, and maintained by community scientists in an effort to promote wildlife monitoring, research, community involvement and education (Townsend et al., 2021). Camera trap networks have the potential to monitor wildlife species diversity on large scales, so long as their limitations and biases are accounted for in diversity indexes. Most camera trap studies implicitly assume that all species are equally detectable (Burton et al., 2015), but detection rates are affected by a number of factors, including body size (Rowcliffe & Carbone, 2008, Tobler et al., 2008), range size (Popescu et al., 2014), heat signature (Welbourne et al., 2016), movement characteristics (Rowcliffe & Carbone, 2008), behavioral response to trail cameras (Hofmeester et al., 2019), and the amount of time spent on the ground for semi-arborial, scansorial, and fossorial species. Camera trap placement (Sollmann et al., 2013) can also favor particular species. Detection rate is affected by detectability and may not be directly related to population density. All these factors bias indices like Shannon diversity.

Furthermore, maximum population density varies greatly by species, sometimes by orders of magnitude. A healthy ecosystem with robust populations would be expected to have higher densities of mice than deer, and higher densities of deer than wolves. Species with larger body mass and at higher trophic levels typically occur at lower densities. Typical diversity indexes, including Shannon (1948), Simpson (1949), and other Hill family indexes (Jost, 2006, Hill, 1973), define an ideal diverse community as one where all species occur at equal densities, and implicitly assume that the maximum population density of all species is the same. In the context of many wildlife studies, but in camera trap networks in particular, the assumptions of equal detectability and equal maximum population density are often violated. In these contexts, using evenness as a component in diversity metrics can produce counterintuitive results.

1.2. A novel index

Here, we present a novel index: Fractional Richness. Fractional Richness goes a step beyond simple species richness in that it accounts for abundances, but unlike typical biodiversity indices which measure the evenness of species, Fractional Richness uses normalized fractional population density (NFPD) to measure how robust or scarce a population is at a particular site in relation to its own maximum population density across sites. Our index weighs all species equally, regardless of population density or detectability, and is intended to replace Hill-family indexes like Shannon diversity in contexts where evenness is uninformative. We use Wisconsin, USA as a case study to compare our index with both Shannon diversity and species richness in their ability to quantify two wildlife communities with different levels of evenness.

1.3. Wisconsin's north–south ecoclimatic and land-use tension zone

Wisconsin has a well-described ecotone between the forested northeast and prairie/savannah southwest (Curtis, 1959), often called a "tension zone" (Livingston, 1903), resulting in distinct plant and animal assemblages in each ecoregion (Temple and Temple, 1986). However, anthropogenic influences also exert a significant impact on species distributions and abundances (Boivin et al., 2016), and recent land use history plays an important role in current mammal distributions in the study region. During pre-colonial times, wolves, black bears, fishers, bobcats, and porcupines occurred throughout Wisconsin (Jackson and Lepage, 1961), but intensive logging and agricultural conversion deforested the majority of the state (Allosso, 2019, Conzen, 2014, Kurta, 1995), causing these forest-dependent species to constrict their ranges northwards. The extensive agricultural conversion of southern Wisconsin caused white-tailed deer and coyotes to become more abundant, led species including eastern cottontails to expand their northern range boundaries, and allowed species like virginia opossums, which had previously never occurred in the state, to flourish (Jackson and Lepage, 1961, Kurta, 1995). Today, Wisconsin is divided more or less north to south, with the north containing intact forest and the south having been converted mostly into settlements and farmland. In addition to the north–south divide in land use, the vegetative ecotone between northern mixed coniferous forests and southern dry prairie-hardwood (Curtis & McIntosh, 1951) coincides with the southern range boundary of mammals like Snowshoe Hares. These southern range boundaries have been creeping northwards through a combination of habitat loss and climate change (Sultaire et al., 2016). This divide creates two semi-distinct wildlife communities within the state, with human-sensitive species being much more abundant in the northern forests, and human-associated species (Gallo et al., 2017) much more abundant in the south. As will be illustrated in the results, attempting to map the diversity of Wisconsin without acknowledging the high turnover in species abundances across this ecotone proves uninformative. For that reason, in this study species were categorized into one of two communities: human-sensitive species in the north, and human-associated species in the south.

1.4. BioCube geospatial layers

Landscape context is central to any analysis of biodiversity indices. A biodiversity index whose assumptions have been violated will not always produce ecologically intuitive values, and as a consequence may not exhibit consistent correlations with ecologically relevant variables across the landscape. If Shannon diversity's assumptions are violated in camera trapping datasets, and if our novel Fractional Richness index is a more effective measurement in the context of camera trap data, then we would expect the predictability of Fractional Richness to be higher than Shannon diversity when modeling that data. To effectively compare diversity across landscapes, it is necessary to account for as many ecologically relevant variables as possible. BioCube (Pavlick et al., 2022) is a geospatially explicit data cube on a common global 1 km grid (WGS-84) that comprises a large collection of ecologically relevant data layers assembled to help predict and understand the distribution and change of various aspects of biodiversity at broad spatial scales. Layers in BioCube have been selected with the prerequisite that they can be produced, or are available, at national to global scales, and that they are related to aspects of biodiversity such as animal species diversity, plant species and functional diversity and patterns of rare and endemic species. BioCube includes several categories of variables that are typically used for biodiversity modeling, such as climate, soil and geology, topography, phenology and anthropogeny. BioCube layers were used to validate the ecological relevance of Fractional Richness as compared to other indices.

1.5. Objectives

In this study we use a network of 2,218 camera traps deployed throughout Wisconsin from 2017–2022 alongside the BioCube, a collection of geospatial data layers assembled to help predict different aspects of biodiversity on a common 1 km grid, to map the diversity of megafauna in Wisconsin, USA. We compare three metrics: Shannon diversity, species richness, and our novel metric Fractional Richness, in their ability to parsimoniously model two semi-distinct wildlife communities with inherently imbalanced species densities. Our key

assumption is that an index that more closely reflects true ecological patterns can be modeled more parsimoniously. Species were subset into those which occur more often in undisturbed habitat (human-sensitive species) and those which occur more often in modified habitat (human-associated species) and the diversity of each of these categories were mapped separately. We hypothesized that Fractional Richness could be modeled more parsimoniously than Shannon diversity, and that the difference would be most evident among human-associated species because that community had a wider range of detection rates.

2. Methods

2.1. Fractional Richness

Our novel index, Fractional Richness, replaces the evenness component typical of most diversity indexes with a measure of normalized fractional population density (NFPD). Where Shannon or Simpson diversity indices define an ideal diverse community as one where many species are equally abundant, Fractional Richness defines an ideal diverse community as one where many species are at high relative population densities. What is considered to be a "high" relative population density differs for each species, based on the average and maximum detection rates of that species across all sites. For example, if bobcats are never detected more often than once per week across all sites, then a site which detects bobcats once a week has a very high relative density of bobcats, but a site that only detects white-tailed deer once per week would have a low relative density of deer if some sites see 20 deer per day. Detection rate for each species at a site (d_{site}) is calculated as the total number of events with the classified species, divided by the total number of days a camera was active at that site. To get the fractional population density for a species, the detection rate at a site is divided by the maximum detection rate for that species across all sites, which means that the density of each species is calculated relative to itself rather than other more- or less-detectable species. Fractional population density for each species is then normalized so that the mean is 0.5, the maximum is 1 and the minimum is zero (Fig. 1). Normalizing the distributions accounts for the right-skewed Poisson distribution typical of camera trap data, while simultaneously ensuring that all species influence the index equally and reducing the impact of high outliers. The mean fractional population density $\overline{\left(\frac{d_{site,i}}{d_{max,i}}\right)}$ is the mean at sites where the species occurs, excluding sites where $d_i = 0$; this ensures that sites outside the species' range or habitat do not skew the mean. The normalized fractional population densities for each species are summed to produce the Fractional Richness for each site (Equation 1). R code for calculating Fractional Richness can be found in the Supplementary Materials and on GitHub (https://github.com/EnSpec/Fractional-Richness). Fractional Richness can be calculated from raw camera trap detection rates with a simple R function; no external data is needed.

$$FractionalRichness_{site} = \sum_{i=1}^{n} \left(\frac{d_{site,i}}{d_{max,i}}\right)^{\frac{\log 0.5}{\log\overline{\left(\frac{d_{site,i}}{d_{max,i}}\right)}}}$$

$\text{FractionalRichness}_{site}$ = Fractional Richness at the site
i = species
n = total number of species
$d_{site,i}$ = detection rate of species i at a site
$d_{max,i}$ = maximum detection rate of species i across sites
$\overline{\left(\frac{d_{site,i}}{d_{max,i}}\right)}$ = mean fractional population density of species i across sites where species i occurs

Fractional Richness behaves differently than Shannon diversity in several key ways:

1. **All species are valued equally.** With Shannon Diversity, low-density or rare species have less impact on the overall diversity score. With Fractional Richness, all species contribute equally to the diversity score (Fig. 2, rows C, D, E).
2. **Fractional Richness increases linearly with species richness.** Shannon Diversity has a plateauing curvilinear distribution, so that the resolution is reduced at higher species richness. Fractional Richness has a linear relationship with species richness and performs equally well at high and low species richness. When all species are at their average population densities, Fractional Richness is equal to ½ species richness. When all species are at their maximum population densities, Fractional Richness is equal to species richness (Fig. 2, rows A, B).
3. **An increase in richness or abundance always results in an increase in Fractional Richness.** With Shannon diversity, if the abundances of species are very uneven, then a decrease in population or a complete loss of the most common species can counterintuitively result in a higher measured diversity (Fig. 2, row C). This is never the case with Fractional Richness.
4. **Population decline results in a loss of Fractional Richness.** If all species become scarce but evenness remains the same, Fractional

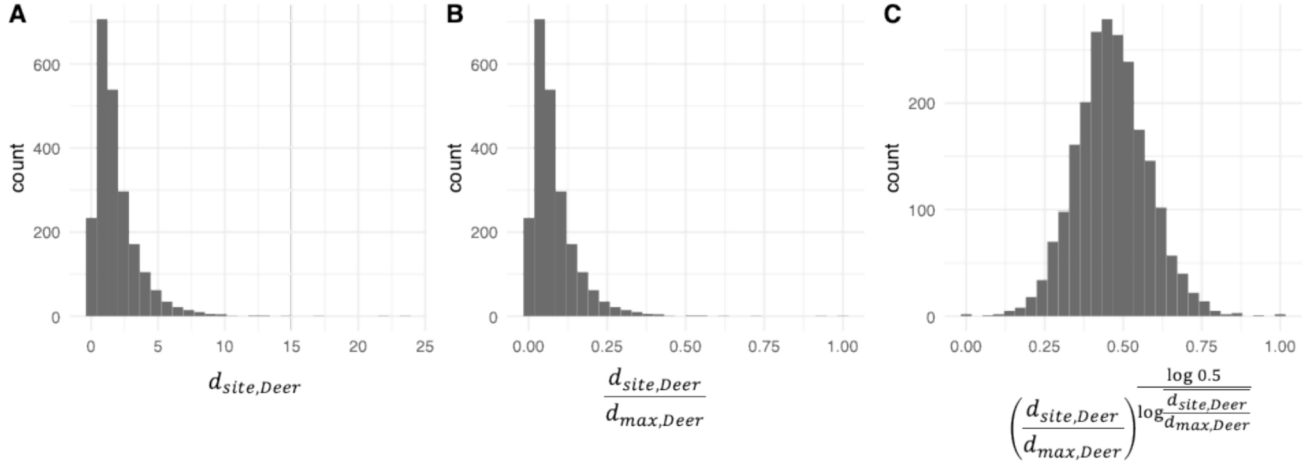

Fig. 1. Visualization of how species detection distributions are normalized. A) Histogram of deer detection rates across sites. The maximum detection rate is 23.51 deer per day, but on average detection rates skew low. B) Fractional population density of deer across sites. Dividing the detection rate at each site by the maximum detection rate fixes the range between 0 and 1. C) Normalized fractional population density (NFPD) of deer across sites. The exponent adjusts the skewness of the distribution, setting the mean fractional population density at 0.5.

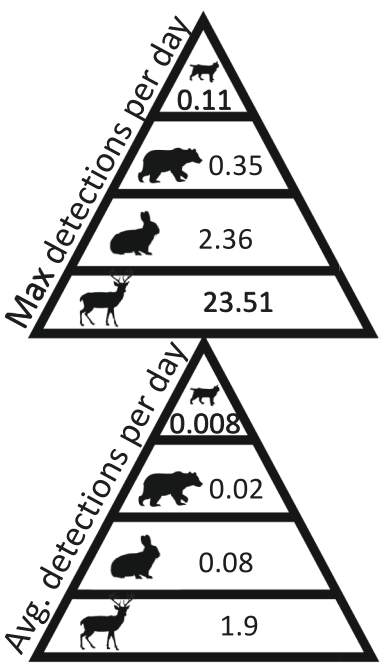

Detections per day at site

					Shannon Diversity	Fractional Richness
A	0.11	0.35	2.36	23.51	0.398	4
B	0.008	0.02	0.08	1.9	0.249	2
C	0.11	0.35	2.36	0	0.535	3
D	0	0.35	2.36	23.51	0.372	3
E	0.11	0.35	0	23.51	0.105	3
F	0.0011	0.0035	0.0236	0.2351	0.398	1.29

$$\left(\frac{0.0011}{0.11}\right)^{\frac{\log 0.5}{\log 0.08}} + \left(\frac{0.0035}{0.35}\right)^{\frac{\log 0.5}{\log 0.06}} + \left(\frac{0.0236}{2.36}\right)^{\frac{\log 0.5}{\log 0.03}} + \left(\frac{0.2351}{23.51}\right)^{\frac{\log 0.5}{\log 0.08}} = 1.29$$

Fig. 2. Case examples of how Shannon Diversity and Fractional Richness behave differently. A) When all species are at their maximum population densities, Fractional Richness is equal to species richness. B) When all species are at their average population densities, Fractional Richness is equal to ½ species richness. C) When population densities are highly uneven and the most common species is lost, Shannon diversity counterintuitively increases. D, E) The loss of a low-density species affects Shannon diversity much less than the loss of a higher-density species. A,F) If all species become scarce but evenness remains the same, Fractional Richness decreases while Shannon diversity remains the same. Values within triangles are the actual maximum detection rates and average detection rates of bobcats, black bears, cottontail rabbits, and white-tailed deer in the Snapshot Wisconsin database.

Richness decreases while Shannon diversity remains constant (Fig. 2, rows A, F).

5. **Species detectability does not bias the index**. Practically speaking, the measured abundance of a species, or its detection rate, is never exactly the same as the true abundance. Some species are more easily detectable than others. Because Fractional Richness values all species equally, and $d_{site,i}$ and $d_{max,i}$ are affected by the same set of biases, species detectability bias is effectively canceled out and does not affect the index, so long as a species that is present is detected.
6. **Multiple sites are required.** The main drawback of Fractional Richness when compared to Shannon diversity is that it requires more information. Shannon diversity can be calculated for a single site, while Fractional Richness requires either multiple sites or multiple time points in order to calculate d_{max} and mean fractional population density.

2.2. Camera trap deployment

A total of 2,218 camera trapping sites (Bushnell TrophyCam models 119,636, 119,836 and 119,837) were established as part of the Snapshot Wisconsin program (Townsend et al., 2021). Cameras were located on both private and public lands throughout the state of Wisconsin, USA, and were deployed and maintained by community scientists. Cameras were affixed to trees 0.75–1 m above the ground, parallel to the ground, facing north when possible, and 10–15 m from a trail. On average, there was one camera for every 30 mi^2 (76 km^2), and cameras were on average about 5 miles (9 km) apart. When motion activated, cameras recorded 3 images in quick succession, each 3-image burst was considered a single event. Wildlife within the images were identified by community scientists maintaining trail cameras, on Zooniverse by community scientists, and more difficult species to identify (e.g., canids, mustelids) were verified by experts. Cameras were not baited. Deployment date and duration varied by camera site. The data collection period ranged from January 1st 2017 until December 31st 2022, a total of 6 years. Each camera site was active for a minimum of one year and had a minimum coverage of 95 %. Coverage (Chao and Jost, 2012, Roswell et al., 2021) is the estimated percentage of species occurring at the site which have been detected, based on the number of singleton detections, and is a measure of whether enough data has been collected to accurately measure richness at a site. Average camera deployment duration was 978 days. Species detection rates (d_{site}) were calculated as the total number of events with the classified species divided by the total number of days a camera was active at that site. d_{max} for each species was the maximum detection rate for that species across all 2,218 camera sites.

2.3. Defining human-sensitive and human-associated species

Species were categorized as human-sensitive or human-associated based on their relationship with Global Human Modification of Terrestrial Ecosystems (GHM, NASA SEDAC v1; Fig. 3). Linear models were made in R to find the relationship between GHM and species detection rate using the formula lm(species ~ GHM), where a negative coefficient estimate indicates a negative relationship with GHM. Coefficient estimates and p-values for each species are available in the Supplementary Materials. Communities included both mammals and large birds, since both were detected frequently in the dataset. This semi-arbitrary community definition was selected primarily as a quantitative way of dividing detected species into two distinct categories. Human-sensitive species were significantly more likely to be detected in less modified habitat and included black bears *Ursus americanus*, beavers *Castor canadensis*, bobcats *Lynx rufus*, fishers *Pekania pennanti*, grey foxes *Urocyon cinereoargenteus*, ruffed grouse *Bonasa umbellus*, North American porcupines *Erethizon dorsatum*, and grey wolves *Canis lupus*. Human-associated species were significantly more likely to be detected in more modified habitat and included eastern cottontail rabbits *Sylvilagus*

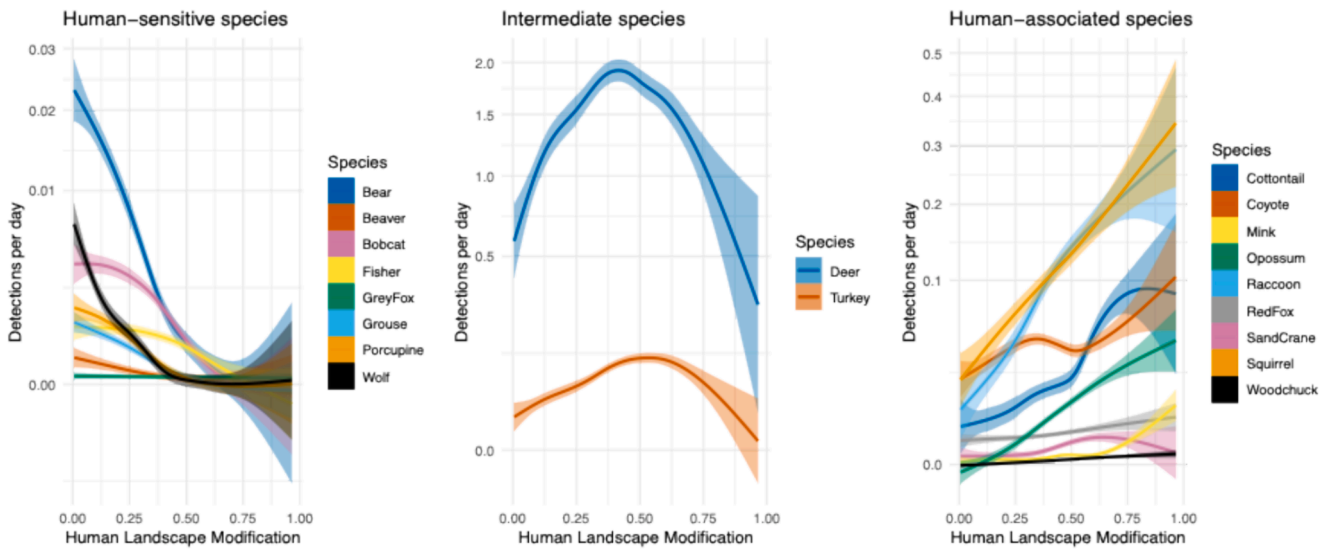

Fig. 3. Relationship between species' detection rates and human landscape modification. Human-sensitive species: species with a significant negative relationship with landscape modification. Human-associated species: species with a significant positive relationship with landscape modification. Intermediate species: species which are most abundant at intermediate levels of landscape modification. The y-axis is on a logarithmic scale to make the lower-density species more visible.

floridanus, coyotes *Canis latrans*, American mink *Neovison vison*, Virginia opossums *Didelphis virginiana*, raccoons *Procyon lotor*, red foxes *Vulpes vulpes*, sandhill cranes *Antigone canadensis*, squirrels *Sciuridae*, and woodchucks *Marmota monax*. Due to the inherent ambiguity of camera trap images in regard to small mammals, squirrels were not identified to species level. Some species, including white-tailed deer *Odocoileus virginianus* and turkeys *Meleagris gallopavo*, did not show a clearly positive or negative correlation with Global Human Modification and were not included in either human-sensitive or human-associated species categories. Overall diversity indices include all species listed here; human-sensitive species, human-associated species, as well as white-tailed deer and turkeys.

2.4. Geospatial predictor variables

Predictor variables used to model biodiversity maps were obtained from BioCube, an open-source data cube framework integrating many geospatial data layers on a shared 1 km raster grid, specifically developed for modeling and understanding biodiversity patterns (Pavlick et al., 2022). Geospatial layer values at camera locations were considered to be the weighted average of pixel values within a 500 m radius of each camera, where weighting was determined by how much of the pixel fell within the 500 m radius. We used a total of 177 geospatial data layers during model selection, see details in the Supplementary Materials. This large contingent of predictor variables was used to ensure that the final models were of the highest possible quality, in order to validate the usefulness of the Fractional Richness index.

We used 71 soil variables from SoilGrids 250 m v2 describing cation exchange capacity, soil nitrogen content, organic carbon density, soil pH, organic carbon density, organic carbon stocks, and proportion of clay, silt, sand, and coarse fragments at depths from 0 cm to 200 cm (SoilGrids, Poggio et al., 2021). We reprojected and regridded the 250 m SoilGrids layers to the 1 km WGS-84 BioCube grid using bilinear resampling. We used 10 topographical variables describing aspect northness, elevation, curvature, roughness, slope and TPI (EarthEnv, Amatulli et al., 2018).

We used 49 bioclimatic variables describing air temperature, seasonality, isothermality, precipitation, growing degree days, snow cover and frost change frequency (CHELSA BioClim v2.1, Karger et al., 2017), potential evapotranspiration, aridity, continentality, emberger's pluviothermic quotient, and thermicity index (ENVIREM, Title and Bemmels, 2018), cloud cover (EarthEnv, Wilson and Jetz, 2016), and MODIS winter habitat indices snow season length, snow cover variability, and percent frozen ground without snow (SILVIS, Zhu et al., 2017, Gudex-Cross et al., 2021) at 1 km, matching the BioCube grid. We used 25 phenological variables describing cumulative, minimum and seasonality of normalized difference vegetation index, enhanced vegetation index, fraction of absorbed photosynthetically active radiation, leaf area index, and gross primary productivity at 1 km (SILVIS, Hobi et al., 2017, Radeloff et al., 2019). As well as the start, end, duration, and amplitude of photosynthetic activity in the canopy at 250 m (USGS EROS 2018, https://doi.org/10.5066/F7PC30G1). We regridded the 250 m USGS phenology layers to the 1 km BioCube grid.

We used 22 anthropogenic variables describing human population count and population density (GPW,CIESIN, 2018), nighttime lights (Li et al., 2020), contextual intactness (Mokany et al., 2020), on-road CO2 emissions (Gately et al. 2019), global human modification of terrestrial systems (Kennedy et al., 2019,2020), biodiversity intactness (Newbold et al., 2016), existing and impacting sound (Mennitt et al., 2014), access to cities (Weiss et al., 2018) and land use proportions categorized into cropland, pasture, primary land cover, secondary land cover, and urban areas (Hoskins et al., 2015,2016), agriculture, built-up, energy production, human intrusions, and transportation (Theobald et al., 2020).

2.5. Model selection

Of the 2,218 camera locations, a random 70 % were sampled without replacement to be used as training data and the remaining 30 % were set aside as test data. Nine models were made: Shannon diversity, species richness, and Fractional Richness, of human-sensitive species, human-associated species, and all species. Due to the computational complexity of performing best subset selection on 177 predictors, the best performing model was chosen from a hybrid stepwise selection. For each diversity metric, geospatial variables were prioritized by making single-variable linear models for each variable and sorting by r-squared, highest r-squared values being first. To make the full model, starting with the variable having the highest r-squared value, variables were added one at a time. After each addition, variables were checked for statistical significance and collinearity, and the updated model was judged based on AIC and accuracy against the test dataset: If the addition of a new variable caused any variable to become insignificant ($p > 0.05$), the least significant variable was removed. If any two spatial

variables in the model were more than 80 % similar, the least significant of the two was removed. If the addition of the new variable did not improve the AIC score, the variable was removed. Predicted values based on training data were compared with measured values from the test dataset, and if correlation between the two did not increase, the newest variable was removed. Variables were added in this manner until all 177 spatial variables had the opportunity to be incorporated into the model. The entire model selection process was executed through a loop code in R using a set seed for randomization of test and training data to ensure the process was reproducible. Most final models had 10 or fewer coefficients. The model selection code is available in the Supplementary Materials.

2.6. Comparison of diversity indexes

It was assumed that a more valid and informative index which reflects true ecological dynamics in the landscape would contain less stochasticity and follow ecologically relevant landscape variables more closely, and therefore could be modeled more parsimoniously. To determine whether one index was significantly and consistently more accurate than another, 10 iterations of each model were made. Training and test data were re-randomized and model selection repeated 10 times to create 10 iterations of each model, for a total of 90 models (3 indices x 3 species communities x 10 iterations). Iterations were used to determine the average model accuracy of each model type. Model accuracy was measured as the correlation between predicted values based on training data and measured values from test data, where higher values indicated higher model accuracy.

3. Results

3.1. Community evenness

The community of human-associated species had highly uneven detection rates between species. The average community evenness across sites was 0.65 (SD = 0.17) and the maximum detection rates ranged across three orders of magnitude. In contrast, the community of human-sensitive species was more even. Average evenness across sites was 0.72 (SD = 0.20) and maximum detection rates stayed primarily within the same order of magnitude (Table 1).

3.2. Model accuracy

Species communities and diversity indices differed in how easily they could be modeled by geospatial variables (Fig. 4). All three diversity indexes could be modeled fairly accurately for Human-sensitive species, but differed significantly in their accuracy for Human-associated species (Fig. 5). Fractional Richness performed significantly better than species richness (*t*-test, p = 1.8e-5) for Human-associated species, while Shannon performed significantly worse than both Fractional Richness (*t*-test, p = 1.8e-5) and Richness (*t*-test, p = 2.6e-7) (Fig. 5). None of the diversity indexes were able to make accurate models of the overall species community: correlation between test data and model predictions was less than 25 % for all models of this type. Best models used 11 or fewer predictor variables. Model summary statistics can be found in the Supplementary Materials.

3.3. Partial dependence of geospatial variables

Human-associated species and Human-sensitive species diversity models showed nearly opposite patterns of diversity (Fig. 6) and were correlated with different geospatial variables. In models using a single variable to predict diversity, climate variables tended to have the highest r-squared values. Overall, the variables which were most frequently incorporated into best models included minimum enhanced vegetative index with quality assessment (EVIQA_2, 30/90 models), mean monthly potential evapotranspiration of the coldest quarter (PETColdQuart, 25/90 models), and seasonality of normalized difference vegetative index (NDVIQA_3, 24/90 models). When modeling human-associated species, the most frequently incorporated variables were NDVIQA_3 (20/30 models), and PETColdQuart (18/30 models), as well as global human modification (18/30 models). For human-sensitive species, the best variables were EVIQA_2 (26/30 models), contextual intactness (15/30 models) and mean daily air temperature of the coldest quarter (15/30 models). Details on specific models and variables are available in the Supplementary Materials.

4. Discussion

Our novel Fractional Richness index is similar to diversity indices in that it incorporates both abundance and species richness information

Table 1
Maximum detection rates and mean fractional population density of each species. Smaller mean fractional population density values indicate a distribution skewed further towards zero. Deer and Turkey are commonly detected species, but were not placed in either the human-associated or human-sensitive species categories because these two species did not have a significant linear relationship with Human Landscape Modification.

	Species	$d_{max,i}$	$\overline{\left(\frac{d_{site,i}}{d_{max,i}}\right)}$	Community Evenness
		Maximum detections per day	Mean Fractional Population Density	
Human-sensitive	Bear	0.35	0.06	Mean = 0.72
	Beaver	0.41	0.07	(SD = 0.20)
	Bobcat	0.11	0.08	
	Fisher	0.24	0.03	
	Grey Fox	0.53	0.02	
	Grouse	0.09	0.07	
	Porcupine	0.17	0.05	
	Wolf	0.64	0.02	
Human-associated	Cottontail	2.36	0.03	Mean = 0.65
	Coyote	0.91	0.07	(SD = 0.17)
	Mink	0.26	0.03	
	Opossum	1.01	0.04	
	Raccoon	6.37	0.03	
	Red Fox	1.23	0.01	
	Sandhill Crane	0.93	0.03	
	Squirrel	3.71	0.06	
	Woodchuck	0.06	0.07	
	Deer	23.51	0.08	
	Turkey	3.35	0.04	

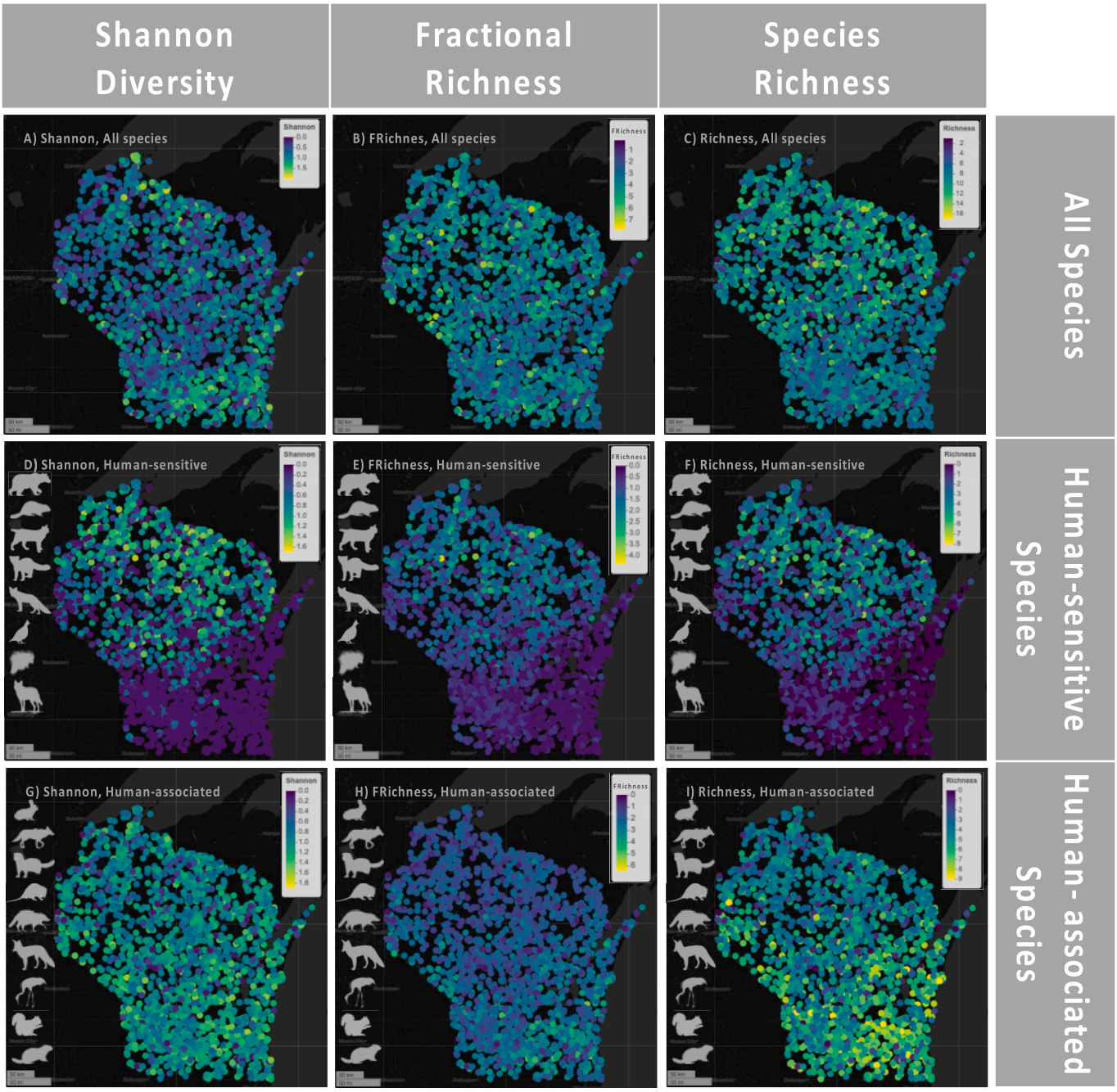

Fig. 4. Raw point maps of A) Shannon diversity of all species, B) Fractional Richness of all species, C) Species richness of all species, D) Shannon diversity of human-sensitive species, E) Fractional Richness of human-sensitive species, F) Species richness of human-sensitive species, G) Shannon diversity of human-associated species, H) Fractional Richness of human-associated species, I) Species richness of human-associated species. Shannon = Shannon diversity. FRichness = Fractional Richness. Richness = species richness. Human-sensitive species include black bear, beaver, bobcat, fisher, grey fox, grouse, porcupine, and grey wolf. Human associated species include cottontail rabbit, coyote, mink, opossum, raccoon, red fox, sandhill crane, squirrel, and woodchuck. 'All species' includes all members of both the human-associated and human-sensitive species communities, plus white-tailed deer and turkey. Each point represents one of the 2,218 camera trap locations. Generated using Mapview v 2.11.2 (Appelhans et al., 2023). (For interpretation of the references to colour in this figure legend, the reader is referred to the web version of this article.)

but differs from true diversity indices because it does not measure the entropy of the system (Jost, 2006). All true diversity indices essentially address the question: when selecting an individual at random from the community, how accurately can one predict the species? Entropy is a useful measure when studying a system like, for example, trees in a forest, where the presence of one species in one location necessarily precludes the presence of another, but wildlife does not saturate the landscape in the same way flora does. Our index fills a similar function to diversity indices, but is mathematically distinct and has properties better attuned to the dynamics of wildlife. Fractional Richness is designed to handle datasets with highly uneven detection rates among species, inherently different population densities due to the presence of multiple trophic levels or a wide range of body sizes, and communities where not all species are equally easily detected. Fractional Richness is also sensitive to population decline.

To assess the ability of our index to handle these sorts of datasets, we looked at two semi-distinct wildlife communities in Wisconsin, USA: human-sensitive species and human-associated species. Of these two

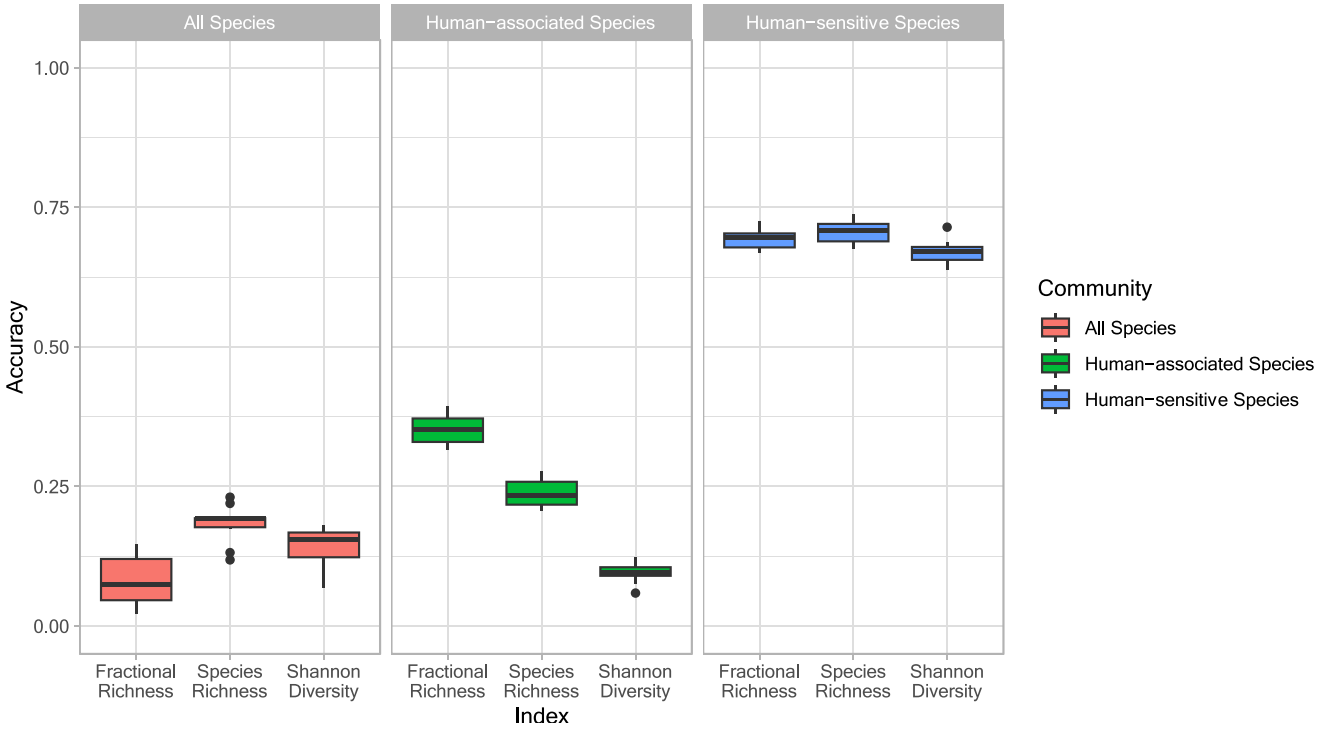

Fig. 5. Accuracy of best models for each diversity index and species cohort. Box plots show accuracy across 10 iterations of each model type. Accuracy is the correlation between measured test data and model predictions.

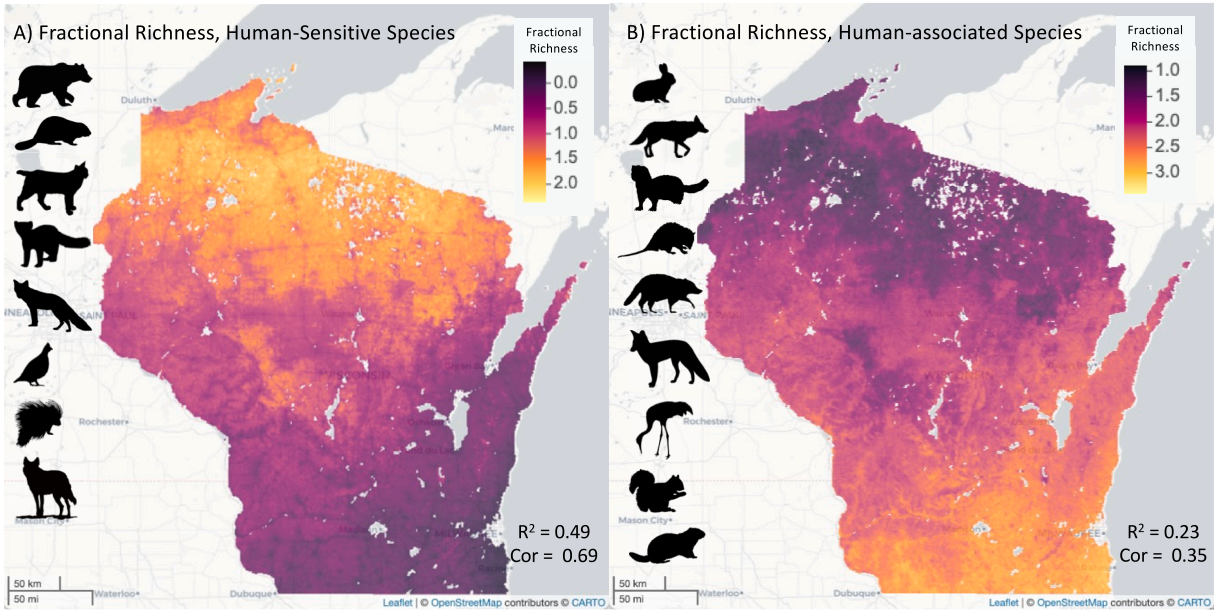

Fig. 6. Predicted Fractional Richness maps of A) Human-sensitive species and B) Human-associated species. Values for each pixel are averaged across 10 model iterations. Human-sensitive species include black bears, beavers, bobcats, fishers, grey foxes, grouse, porcupines, and wolves. Human-associated species include cottontail rabbits, coyotes, minks, opossums, raccoons, red foxes, sandhill cranes, squirrels, and woodchucks. Fractional Richness is equal to ½ species richness when all species are at average population density. Pixels from built-up urban areas and water bodies were excluded from the prediction. Cor = average Pearson's correlation between predicted values and measured test data of the 10 model iterations. R^2 = average r-squared of the 10 model iterations. Generated using Mapview v 2.11.2 (Appelhans et al., 2023). (For interpretation of the references to colour in this figure legend, the reader is referred to the web version of this article.)

communities, human-associated species had a less obvious pattern of diversity across the landscape (Fig. 4), and had a more severe case of the complications which make evenness, and by extension Hill family indexes like Shannon diversity, less informative: Maximum detection rates ranged across three orders of magnitude (Fig. 2, Table 1) and were significantly impacted by how easily each species was detectable by camera traps. These same complications were present among the community of human-sensitive species, but to a lesser extent.

We modeled Shannon diversity, Fractional Richness, and Species richness of human-sensitive species, human-associated species, and the overall species community, under the assumption that a diversity index that more accurately reflects true ecological patterns should be able to

be modeled more parsimoniously. Fractional Richness could accurately be modeled for the highly uneven community of human-associated species, while Shannon diversity could not.

4.1. When imbalance is minor, traditional indexes work well

The community of human-sensitive species exhibited very clear differences in diversity across the landscape (Fig. 4). Many species were entirely absent from the southern reaches of the state, which allowed geospatial patterns to be modeled quite well with simple species richness, even before considering the abundance components of Shannon diversity (evenness) and Fractional Richness (NFPD). Because the richness component of the indices played a prominent role in this context, the differences between indices were less evident. All three indexes showed a north–south pattern which was clear even in the raw point data before modeling. All three indexes, including Shannon, could be modeled parsimoniously (Fig. 5), reflecting that the signal-to-noise ratio was comparatively high. The stochasticity introduced by idiosyncrasies of the diversity metric or other factors was small compared to the overall trend in diversity across the landscape. Shannon's index is one of the most popular diversity indexes implemented in ecology and has successfully produced informative results across countless studies for decades. Other Hill family diversity indexes, including Simpson's index and the Berger-Parker index, are similarly valuable (Keylock, 2005). Shannon diversity assumes that sampling is not biased towards any species and that all species have the same maximum population density. When these assumptions are violated, as they often are in wildlife and camera trapping studies, it may be more appropriate to use an alternative index.

4.2. When imbalance is severe, evenness can be detrimental

For our more imbalanced community (human-associated species), the pattern of diversity across the landscape was more nuanced, with a lower signal-to-noise ratio, making it more difficult to accurately model diversity. In this more-difficult-to-model community the differences between indices can be seen more clearly. Shannon diversity performed significantly worse than both simple species richness (*t*-test, p = 2.6e-7) and Fractional Richness (*t*-test, p = 1.8e-5, Fig. 5), suggesting that the evenness component of the index, rather than contributing useful information, may have instead introduced an element of stochasticity. Shannon diversity can behave counterintuitively when species are highly uneven (Fig. 2), or when evenness is biased by detectability.

4.3. When imbalance is severe, Fractional Richness provides an effective measure of diversity

Fractional Richness performed significantly better than both richness and Shannon diversity for our highly imbalanced community (human-associated species), suggesting that Fractional Richness is indeed robust to many of the complications in the dataset which make evenness less informative (Fig. 5), and is able to take species detection rates into account in an ecologically informative way even when detectability and maximum population density vary by species.

4.4. Human-associated species and human-sensitive species had opposite patterns of diversity

The predicted diversity maps of human-sensitive and human-associated species were nearly inverse of each other (Fig. 6), with sensitive species most diverse in northern WI and associated species most diverse in southern WI. Most likely, this inverse pattern was the reason model accuracy of the overall species community was low across all index types (Fig. 5).

4.5. Comparison with other diversity indexes

There are other biodiversity indexes which account for species abundances without using evenness, similar to Fractional Richness. The Biodiversity Intactness Index (BII, Scholes & Biggs, 2005), the Natural Capital Index (NCI, Ten Brink, 2003), the IUCN Red List Index (Baillie et al., 2008, Butchart et al., 2004,2007), the Living Planet Index (Loh et al., 2005), and the Wild Bird Index (Gregory et al., 2003,2005,2008) all measure current abundances as a ratio against some baseline, such as pre-industrial population density, to estimate the degree of population decline. However, unlike Fractional Richness, these indexes require external data or expert opinion to estimate what the detection rate of a robust population should be, and cannot be calculated from raw camera trap data. Using historical population densities as a baseline can be useful in the context of some conservation-oriented studies, and while Fractional Richness does not require this kind of external data, the estimated detection rate at historic densities can be used in place of d_{max} to show how population has declined over time.

There are also existing biodiversity indexes designed for use with camera trap data, most notably the Wildlife Picture Index (WPI, O'Brien et al., 2010). WPI is the average increase or decrease in detection rates across species compared to the detection rate during the first year of data collection. Neither WPI nor Fractional Richness uses evenness, avoiding the issue of variable detectability between species. However, Fractional Richness has a number of features that WPI lacks. WPI focuses on changes in population density and poorly handles differences in richness. WPI depends on arbitrary near-zero placeholder values to produce valid results when zeros occur in a dataset (O'Brien et al., 2010) – zeros occur any time a species is present at some sites but not others, or when a species goes extinct or is introduced partway through the time series. The other major differences between these indexes may be due to their slightly different intended uses: WPI was designed for time series data, to track changes in a single site over time, while Fractional Richness is designed to effectively compare many sites. Only Fractional Richness normalizes the poisson distribution typical of camera trap data, but this correction is less necessary when analyzing data from a single site.

4.6. Assumptions of the index

Fractional Richness assumes that there are robust populations of each species somewhere within the network of study sites, but if habitat is degraded throughout the network of sites, or if the network contains only marginal habitat for some species, then the measured d_{max} may not reflect true maximum population density. This sometimes-flawed assumption generally only becomes problematic when comparing Fractional Richness values calculated separately using different values of d_{max} for the same species. It is better to recalculate Fractional Richness if additional sites are added to the network, especially if population densities are higher at the new sites. For example, if one study measured Fractional Richness for a camera trap network in Yellowstone National Park, WY, and another measured Fractional Richness in Wisconsin, these studies might have different d_{max} values for wolves, and comparing wolf NFPD values without using a shared d_{max} could give the false impression that wolf populations in Yellowstone and Wisconsin are the same. The best practice approach would be to treat all sites as if they belonged to the same network and recalculate d_{max} for each species.

Fractional Richness also assumes that all cameras have equal detection capabilities. Factors like field of view, proximity to game trails, and trigger sensitivity can introduce stochasticity when they differ between cameras. In situations where, for example, some cameras are deployed in grasslands with a very large field of view, and other cameras are deployed in dense forest with a very small field of view, Fractional Richness estimates may be biased towards grassland habitat if field of view is not accounted for. In our camera trap network, all cameras were deployed in forest and had fields of view that were similar, but not identical. All cameras were of the same model, using the same settings,

and were deployed using a uniform protocol. Nevertheless, camera trap placement inevitably influenced the detection rate at individual cameras to some extent and may account for some of the stochasticity in the data which could not be predicted by any model.

It is also assumed that detection rate is a function of population density. However, behavior and activity also influence camera trap detection rates. When calculating Fractional Richness care should be taken to ensure that the periods of data collection are comparable across sites in regard to diel and seasonal cycles. For example, camera traps that were active only during the summer would be expected to have higher detection rates of bears than camera traps which were active only during the winter.

4.7. Conceptual issues

Fractional Richness measures the effective richness of a community, and defines a healthy biodiverse ecosystem as one which can support the most species at the highest densities. It does not account for situations where species presence or high density is undesirable. The presence of an invasive species can cause Fractional Richness to increase, so long as that invasive species does not cause population declines or extirpation of any other species. Species that tend towards overpopulation will contribute most to the Fractional Richness value at sites where their population is highest, and again can cause Fractional Richness to increase so long as the overpopulation of that species does not cause decline in any other species.

Fractional Richness also values all species equally. This is generally seen as a strength of the index, but from a conservation perspective certain species may be valued more than others. In the context of conservation work, it may be appropriate to selectively exclude species which are associated with human disturbance, as they frequently have distributions distinct from species of higher conservation priority (Fig. 6, Dobson et al., 1997). In Wisconsin, most species of conservation priority, such as grey wolves and fishers, were most abundant in the less disturbed northern reaches of the state. While species of low conservation concern like raccoons and Virginia opossums had a nearly opposite pattern of abundance. Attempting to measure the diversity of the overall species community failed to reveal any spatial pattern of high-diversity habitat across the state (Fig. 4) because the northern and southern communities effectively balance each other. In order to use Fractional Richness in an ecologically informative way, it is still necessary to have a knowledge of factors such as ecotones which influence the ecosystem being analyzed.

Fractional Richness uses the average detection rate of a species to adjust the skewness of the distribution. This is something to keep in mind if using time-series data, especially for species in decline, because the historic average population density of a species is often different from the overall average population density of a species. Consider, for example, a reintroduction effort in a park where fishers were nearly extirpated 20 years ago. The average detection rate of fishers over the last 20 years would be significantly lower than the average rate more than 20 years ago. Managers might prefer to use only the historical average detection rate from more than 20 years ago when judging the effectiveness of their reintroduction efforts. When a species is at a low population density for a long time, the average detection rate tends to decrease, which can lead the index to treat intermediate values more favorably.

5. Conclusions

Fractional Richness is a novel biodiversity metric intended for use with large camera trap networks. It uses normalized fractional population density (NFPD) rather than evenness to account for species detection rates. Fractional Richness is highest when a large number of species are at their maximum population densities, and increases linearly with species richness. It normalizes the Poisson distribution typical of camera trap data rather than assuming population density will be directly proportional to detection rate. Fractional Richness provides robust, ecologically relevant biodiversity estimates even when detectability varies by species, or when maximum population density varies by orders of magnitude between species. To the best of our knowledge, this is the only diversity index to do so without depending on large amounts of external data or expert opinion.

6. Statement on Inclusion

Our study includes authors based in the country where the study was carried out.

Author Contributions

Laura Marie Berman and Philip Townsend conceived the ideas. Fabian D Schneider and Morgan Dean curated BioCube data. Jennifer Stenglein and Ryan Bemowski curated Snapshot Wisconsin data. Laura Marie Berman developed the index and conducted the formal analysis. Fabian D Schneider, Ryan P Pavlick and Philip Townsend acquired funding. Philip Townsend supervised. Laura Marie Berman wrote the original draft. All authors contributed towards the review and editing of the final manuscript.

CRediT authorship contribution statement

Laura Marie Berman: Writing – review & editing, Writing – original draft, Visualization, Validation, Methodology, Formal analysis, Conceptualization. **Fabian D Schneider:** Writing – review & editing, Funding acquisition, Data curation. **Ryan P. Pavlick:** Writing – review & editing, Funding acquisition. **Jennifer Stenglein:** Writing – review & editing, Data curation. **Ryan Bemowski:** Writing – review & editing, Data curation. **Morgan Dean:** Writing – review & editing, Data curation. **Philip A Townsend:** Writing – review & editing, Supervision, Funding acquisition, Conceptualization.

Declaration of competing interest

The authors declare that they have no known competing financial interests or personal relationships that could have appeared to influence the work reported in this paper.

Data availability

Code used to calculate Fractional Richness and camera trap data used in this article are available on github (https://github.com/EnSpec/Fractional-Richness). Camera traps in the Snapshot Wisconsin network are maintained by community scientists on private land. To protect the privacy of these community scientists, latitude has been coarsened to two decimal places and longitude has been coarsened to one decimal place, reducing location precision to within 5 km in the publicly available dataset. All geospatial data layers are publicly available.

Acknowledgements

This research was funded by a NASA Biodiversity Program grant (BIODIV 2020) to JPL and the University of Wisconsin-Madison. The research carried out by FDS and RPP at the Jet Propulsion Laboratory, California Institute of Technology, was under a contract with the National Aeronautics and Space Administration (80NM0018D0004). Additional support was provided by annual USFWS Federal Aid in Wildlife Restoration Grants to the Wisconsin Department of Natural Resources. Thank you to the thousands of Snapshot Wisconsin volunteers who were essential to data collection and processing, including trail camera hosts and Zooniverse photo classifiers. Wisconsin Department of Natural Resources Office of Applied Science staff were pivotal in

training and supporting volunteers and developing photo work flows and classification procedures. This publication uses data generated via the Zooniverse.org platform, funded in part by a grant from the Alfred P. Sloan Foundation. Aspects of this research have also received support from NASA Ecological Forecasting (NNX14AC36G) and NASA ESSF (NNX16A061H) programs, as well as the NSF ASCEND Biology Integration Institute (BII) through DBI award 2021898 to PAT.

Appendix A. Supplementary data

Supplementary data to this article can be found online at https://doi.org/10.1016/j.ecolind.2024.112266.

References

Ahumada, J.A., Silva, C.E., Gajapersad, K., Hallam, C., Hurtado, J., Martin, E., Andelman, S.J., 2011. Community structure and diversity of tropical forest mammals: data from a global camera trap network. Philos. Trans. r. Soc., B 366 (1578), 2703–2711. https://doi.org/10.1098/rstb.2011.0115.

Allosso, D. (2019). American Environmental History.

Amatulli, G., Domisch, S., Tuanmu, M.N., Parmentier, B., Ranipeta, A., Malczyk, J., Jetz, W., 2018. A suite of global, cross-scale topographic variables for environmental and biodiversity modeling. Sci. Data 5 (1), 1–15. https://doi.org/10.1038/sdata.2018.40.

Appelhans, T., Detsch, F., Reudenbach, C., Woellauer, S., 2023. mapview: interactive Viewing of Spatial Data in R. R Package Version 2 (11), 2. https://github.com/r-spatial/mapview.

Baillie, J.E., Collen, B., Amin, R., Akcakaya, H.R., Butchart, S.H., Brummitt, N., Mace, G. M., 2008. Toward monitoring global biodiversity. Conserv. Lett. 1 (1), 18–26. https://doi.org/10.1111/j.1755-263X.2008.00009.x.

Boivin, N.L., Zeder, M.A., Fuller, D.Q., Crowther, A., Larson, G., Erlandson, J.M., Petraglia, M.D., 2016. Ecological consequences of human niche construction: examining long-term anthropogenic shaping of global species distributions. Proc. Natl. Acad. Sci. 113 (23), 6388–6396. https://doi.org/10.1073/pnas.1525200113.

Burton, A.C., Neilson, E., Moreira, D., Ladle, A., Steenweg, R., Fisher, J.T., Boutin, S., 2015. Wildlife camera trapping: a review and recommendations for linking surveys to ecological processes. J. Appl. Ecol. 52 (3), 675–685. https://doi.org/10.1111/1365-2664.12432.

Butchart, S.H., Resit Akçakaya, H., Chanson, J., Baillie, J.E., Collen, B., Quader, S., Hilton-Taylor, C., 2007. Improvements to the red list index. PLoS One 2 (1), e140.

Butchart, S.H.M., Stattersfield, A.J., Bennun, L.A., Shutes, S.M., Akçakaya, H.R., Baillie, J.E.M., Mace, G.M., 2004. Measuring global trends in the status of biodiversity: red List Indices for birds. PLoS Biol. 2 (12), e383.

Chao, A., Jost, L., 2012. Coverage-based rarefaction and extrapolation: standardizing samples by completeness rather than size. Ecology 93 (12), 2533–2547. https://doi.org/10.1890/11-1952.1.

Conzen, M.P., 2014. The making of the American landscape. Routledge. https://doi.org/10.4324/9781315810829.

Cove, M.V., Kays, R., Bontrager, H., Bresnan, C., Lasky, M., Frerichs, T., Jordan, M.J., 2021. SNAPSHOT USA 2019: a coordinated national camera trap survey of the United States. Ecology 102 (6). https://doi.org/10.1002/ecy.3353.

Curtis, J.T., 1959. The vegetation of Wisconsin: an ordination of plant communities. University of Wisconsin Pres.

Curtis, J.T., McIntosh, R.P., 1951. An upland forest continuum in the prairie-forest border region of Wisconsin. Ecology 32 (3), 476–496. https://doi.org/10.2307/1931725.

Dobson, A.P., Rodriguez, J.P., Roberts, W.M., Wilcove, D.S., 1997. Geographic distribution of endangered species in the United States. Science 275 (5299), 550–553. https://doi.org/10.1126/science.275.5299.550.

Gallo, T., Fidino, M., Lehrer, E.W., Magle, S.B., 2017. Mammal diversity and metacommunity dynamics in urban green spaces: implications for urban wildlife conservation. Ecol. Appl. 27 (8), 2330–2341. https://doi.org/10.1002/eap.1611.

Center for International Earth Science Information Network - CIESIN - Columbia University. (2018). *Gridded Population of the World, Version 4.11 (GPWv4),* Revision 11. Palisades, NY: NASA Socioeconomic Data and Applications Center (SEDAC). 10.7927/H4JW8BX5.

Gregory, R. D., Vorišek, P., Noble, D. G., Van Strien, A., Klvaňová, A., Eaton, M., ... & Burfield, I. J. (2008). The generation and use of bird population indicators in Europe. *Bird Conservation International*, *18*(S1), S223-S244. 10.1017/S0959270908000312.

Gregory, R.D., Noble, D., Field, R., Marchant, J., Raven, M., Gibbons, D.W., 2003. Using birds as indicators of biodiversity. Ornis Hungarica 12 (13), 11–24.

Gregory, R.D., Van Strien, A., Vorisek, P., Gmelig Meyling, A.W., Noble, D.G., Foppen, R. P., Gibbons, D.W., 2005. Developing indicators for European birds. Philos. Trans. r. Soc., B 360 (1454), 269–288. https://doi.org/10.1098/rstb.2004.1602.

Gudex-Cross, D., Keyser, S.R., Zuckerberg, B., Fink, D., Zhu, L., Pauli, J.N., Radeloff, V.C., 2021. Winter Habitat Indices (WHIs) for the contiguous US and their relationship with winter bird diversity. Remote Sens. Environ. 255, 112309 https://doi.org/10.1016/j.rse.2021.112309.

Hill, M.O., 1973. Diversity and evenness: a unifying notation and its consequences. Ecology 54 (2), 427–432. https://doi.org/10.2307/1934352.

Hobi, M.L., Dubinin, M., Graham, C.H., Coops, N.C., Clayton, M.K., Pidgeon, A.M., Radeloff, V.C., 2017. A comparison of Dynamic Habitat Indices derived from different MODIS products as predictors of avian species richness. Remote Sens. Environ. 195, 142–152. https://doi.org/10.1016/j.rse.2017.04.018.

Hofmeester, T.R., Cromsigt, J.P., Odden, J., Andrén, H., Kindberg, J., Linnell, J.D., 2019. Framing pictures: a conceptual framework to identify and correct for biases in detection probability of camera traps enabling multi-species comparison. Ecol. Evol. 9 (4), 2320–2336. https://doi.org/10.1002/ece3.4878.

Hoskins, A.J., Bush, A., Gilmore, J., Harwood, T., Hudson, L.N., Ware, C., Ferrier, S., 2016. Downscaling land-use data to provide global 30 ″estimates of five land-use classes. Ecol. Evol. 6 (9), 3040–3055. https://doi.org/10.1002/ece3.2104.

Hoskins, Andrew; Bush, Alex; Gilmore, James; Harwood, Tom; Ware, Chris; Williams, Kristen; Ferrier, Simon (2015): Global 30s resolution land use for 2005. v3. CSIRO. Data Collection. 10.4225/08/56DCD9249B224.

Jackson, H.H.T., Lepage, J., 1961. Mammals of Wisconsin. University of Wisconsin Press, United Kingdom.

Jost, L., 2006. Entropy and diversity. Oikos 113 (2), 363–375. https://doi.org/10.1111/j.2006.0030-1299.14714.x.

Karger, D.N., Conrad, O., Böhner, J., Kawohl, T., Kreft, H., Soria-Auza, R.W., Zimmermann, N.E., Linder, P., Kessler, M., 2017. Climatologies at high resolution for the Earth land surface areas. Sci. Data 4, 170122. https://doi.org/10.1038/sdata.2017.122.

Karger D.N., Conrad, O., Böhner, J., Kawohl, T., Kreft, H., Soria-Auza, R.W., Zimmermann, N.E,, Linder, H.P., Kessler, M.. Data from: Climatologies at high resolution for the earth's land surface areas. Dryad Digital Repository.https://doi.org/doi:10.5061/dryad.kd1d4.

Kennedy, C. M., Oakleaf, J. R., Theobald, D. M., Baruch-Mordo, S., & Kiesecker, J. (2019). Managing the middle: A shift in conservation priorities based on the global human modification gradient. *Global Change Biology*, *25*(3), 811-826. 10.1111/gcb.14549.

Kennedy, C. M., Oakleaf, J. R., Theobald, D. M., Baruch-Mordo, S., & Kiesecker, J. (2020). Documentation for the global human modification of terrestrial systems. *NASA Socioeconomic Data and Applications Center (SEDAC): Palisades, NY, USA*. 10.7927/edbc-3z60.

Keylock, C., 2005. Simpson diversity and the Shannon-Wiener index as special cases of a generalized entropy. Oikos 109 (1), 203–207. https://doi.org/10.1111/j.0030-1299.2005.13735.x.

Kurta, A., 1995. Mammals of the Great Lakes Region. University of Michigan Press, United States.

Li, X., Zhou, Y., Zhao, M., Zhao, X., 2020. A harmonized global nighttime light dataset 1992–2018. Sci. Data 7 (1), 168. https://doi.org/10.1038/s41597-020-0510-y.

Livingston, B.E., 1903. The distribution of the upland plant societies of Kent County. Michigan. *Botanical Gazette* 35 (1), 36–55.

Loh, J., Green, R.E., Ricketts, T., Lamoreux, J., Jenkins, M., Kapos, V., Randers, J., 2005. The Living Planet Index: using species population time series to track trends in biodiversity. Philos. Trans. r. Soc., B 360 (1454), 289–295. https://doi.org/10.1098/rstb.2004.1584.

McShea, W.J., Forrester, T., Costello, R., He, Z., Kays, R., 2016. Volunteer-run cameras as distributed sensors for macrosystem mammal research. Landsc. Ecol. 31, 55–66. https://doi.org/10.1007/s10980-015-0262-9.

Mennitt, D., Fristrup, K. M., & Nelson, L. (2014). Mapping the extent of noise on a national scale.

Mokany, K., Ferrier, S., Harwood, T.D., Ware, C., Di Marco, M., Grantham, H.S., Watson, J.E., 2020. Reconciling global priorities for conserving biodiversity habitat. Proc. Natl. Acad. Sci. 117 (18), 9906–9911. https://doi.org/10.1073/pnas.1918373117.

Newbold, T., Hudson, L.N., Arnell, A.P., Contu, S., De Palma, A., Ferrier, S., Purvis, A., 2016a. Has land use pushed terrestrial biodiversity beyond the planetary boundary? A Global Assessment. *Science* 353 (6296), 288–291. https://doi.org/10.1126/science.aaf2201.

Newbold, Tim; Lawrence Hudson; Andy Arnell; Sara Contu et al. (2016). *Global map of the Biodiversity Intactness Index, from Newbold et al. (2016) Science* . Natural History Museum. 10.5519/0009936.

O'Brien, T.G., Baillie, J.E.M., Krueger, L., Cuke, M., 2010. The Wildlife Picture Index: monitoring top trophic levels. Anim. Conserv. 13 (4), 335–343. https://doi.org/10.1111/j.1469-1795.2010.00357.x.

Pavlick, R., Schneider, F. D., Townsend, P. A., Zheng, T., Queally, N., & Ye, Z. (2022, December). BioCube: Mapping and integrating remote-sensing and in-situ dimensions of biodiversity at large scales. In *AGU Fall Meeting Abstracts* (Vol. 2022, pp. B15A-04).

Poggio, L., De Sousa, L.M., Batjes, N.H., Heuvelink, G., Kempen, B., Ribeiro, E., Rossiter, D., 2021. SoilGrids 2.0: producing soil information for the globe with quantified spatial uncertainty. Soil 7 (1), 217–240. https://doi.org/10.5194/soil-7-217-2021.

Popescu, V.D., de Valpine, P., Sweitzer, R.A., 2014. Testing the consistency of wildlife data types before combining them: the case of camera traps and telemetry. Ecol. Evol. 4 (7), 933–943. https://doi.org/10.1002/ece3.997.

Radeloff, V.C., Dubinin, M., Coops, N.C., Allen, A., Brooks, T.M., Clayton, M., Costa, G., Graham, C.H., Helmers, D., Ives, A.R., Kolesov, D., Pidgeon, A.M., Rapacciuolo, G., Razenkova, E., Suttidate, N., Young, B.E., Zhu, L., Hobi, M., 2019. The Dynamic Habitat Indices (DHIs) from MODIS and global biodiversity. Remote Sens. Environ. 222, 204–214. https://doi.org/10.1016/j.rse.2018.12.009.

Roswell, M., Dushoff, J., Winfree, R., 2021. A conceptual guide to measuring species diversity. Oikos 130 (3), 321–338. https://doi.org/10.1111/oik.07202.

Rowcliffe, J.M., Carbone, C., 2008. Surveys using camera traps: are we looking to a brighter future? Anim. Conserv. 11 (3), 185–186. https://doi.org/10.1111/j.1469-1795.2008.00180.x.

Scholes, R.J., Biggs, R., 2005. A biodiversity intactness index. Nature 434 (7029), 45–49. https://doi.org/10.1038/nature03289.

Shannon, C.E., 1948. A mathematical theory of communication. Bell Syst. Tech. J. 27 (3), 379–423.

Simpson, E. H. (1949). Measurement of diversity. *nature*, *163*(4148), 688-688.

Sollmann, R., Mohamed, A., Samejima, H., Wilting, A., 2013. Risky business or simple solution–Relative abundance indices from camera-trapping. Biol. Conserv. 159, 405–412. https://doi.org/10.1016/j.biocon.2012.12.025.

Steenweg, R., Hebblewhite, M., Kays, R., Ahumada, J., Fisher, J.T., Burton, C., Rich, L.N., 2017. Scaling-up camera traps: monitoring the planet's biodiversity with networks of remote sensors. Front. Ecol. Environ. 15 (1), 26–34. https://doi.org/10.1002/fee.1448.

Sultaire, S.M., Pauli, J.N., Martin, K.J., Meyer, M.W., Zuckerberg, B., 2016. Extensive forests and persistent snow cover promote snowshoe hare occupancy in Wisconsin. J. Wildl. Manag. 80 (5), 894–905. https://doi.org/10.1002/jwmg.21083.

Temple, S.A., Temple, A.J., 1986. Geographic distribution and patterns of relative abundance of Wisconsin birds: a WSO research project. Passenger Pigeon 48, 58–68.

Ten Brink, B. J. E., Van Hinsberg, A., De Heer, M., de Knegt, B., Knol, O. M., Ligtvoet, W., ... & Reijnen, M. J. S. M. (2003). Technisch ontwerp Natuurwaarde 1.0 en toepassing in Natuurverkenning 2. http://hdl.handle.net/10029/9192.

Theobald, D.M., Kennedy, C., Chen, B., Oakleaf, J., Baruch-Mordo, S., Kiesecker, J., 2020. Earth transformed: detailed mapping of global human modification from 1990 to 2017. Earth Syst. Sci. Data 12 (3), 1953–1972. https://doi.org/10.5194/essd-12-1953-2020.

Title, P.O., Bemmels, J.B., 2018. ENVIREM: an expanded set of bioclimatic and topographic variables increases flexibility and improves performance of ecological niche modeling. Ecography 41 (2), 291–307. https://doi.org/10.1111/ecog.02880.

Tobler, M.W., Carrillo-Percastegui, S.E., Leite Pitman, R., Mares, R., Powell, G., 2008. An evaluation of camera traps for inventorying large-and medium-sized terrestrial rainforest mammals. Anim. Conserv. 11 (3), 169–178. https://doi.org/10.1111/j.1469-1795.2008.00169.x.

Townsend, P.A., Clare, J.D., Liu, N., Stenglein, J.L., Anhalt-Depies, C., Van Deelen, T.R., Zuckerberg, B., 2021. Snapshot Wisconsin: networking community scientists and remote sensing to improve ecological monitoring and management. Ecol. Appl. 31 (8), e02436 https://doi.org/10.1002/eap.2436.

Weiss, D.J., Nelson, A., Gibson, H.S., Temperley, W., Peedell, S., Lieber, A., Gething, P. W., 2018. A global map of travel time to cities to assess inequalities in accessibility in 2015. Nature 553 (7688), 333–336. https://doi.org/10.1038/nature25181.

Welbourne, D.J., Claridge, A.W., Paull, D.J., Lambert, A., 2016. How do passive infrared triggered camera traps operate and why does it matter? Breaking down common misconceptions. Remote Sens. Ecol. Conserv. 2 (2), 77–83. https://doi.org/10.1002/rse2.20.

Wilson, A.M., Jetz, W., 2016. Remotely sensed high-resolution global cloud dynamics for predicting ecosystem and biodiversity distributions. PLoS Biol 14 (3), e1002415, 10.1371/journal. pbio.1002415" Data available online at http://www.earthenv.org/.

Wilson, A.M., Jetz, W., 2016. Remotely Sensed High-Resolution Global Cloud Dynamics for Predicting Ecosystem and Biodiversity Distributions. PLoS Biol 14 (3), e1002415. https://doi.org/10.1371/journal.pbio.1002415.

Zhu, L., Radeloff, V.C., Ives, A.R., 2017. Characterizing global patterns of frozen ground with and without snow cover using microwave and MODIS satellite data products. Remote Sens. Environ. 191, 168–178. https://doi.org/10.1016/j.rse.2017.01.020.